

Smith Predictor-based Adaptive Control of Network-Controlled UAVs

Antonio Silveira* Lucas Sodré* Anderson Silva*
Lucas Conde** João Borges** Yuri Souza**
Aldebaro Klautau**

* *Laboratório de Controle e Sistemas, Universidade Federal do Pará, PA, (e-mail: asilveira@ufpa.br, lucas.sodre@itec.ufpa.br, anso@ufpa.br).*

** *Núcleo de P&D em Telecomunicações, Automação e Eletrônica, Universidade Federal do Pará, PA (e-mail: lucas.conde@itec.ufpa.br, joao.tavares.borges@itec.ufpa.br, yuri.souza@itec.ufpa.br, aldebaro@ufpa.br)*

Abstract: Assuming an imminent futuristic scenario, of 5G-and-Beyond communications networks, where different classes of autonomous unmanned aerial vehicles will use guidance, navigation and control systems relying on the network's performance, in this paper we investigate the delay and packet loss effects which may lead to closed-loop stability margins degradation of such aerial vehicles, causing accidents. The use of state observers can minimize these adverse effects by allowing these control systems to receive estimated data whenever sensor data is delayed or lost. In this sense, we propose the assessment of a Smith predictor-based self-tuning control applied to a 6-DOF model of a network-controlled quadrotor. The investigation is focused on Proportional-Integral-Derivative control due to its solid acceptance as a trustworthy industrial technique. Simulations and robustness indices indicates that the investigated control approach can guarantee the robust stability of such aerial systems within the considered scenario.

Keywords: UAV, Smith predictor, adaptive control, mobile-enabled UAV control.

1. INTRODUCTION

In this work we focus on a particular problem in autonomous guidance of aerial vehicles: the network latency and packet loss influence on the closed-loop control dynamics for an ever-increasing number of vehicles in a futuristic urban air mobility network.

Unmanned aerial vehicles (UAV) of the quadrotor type, commonly known as drones, are being commercialized for entertainment activities and are increasing the aerial space occupation in populated zones. Also, the prospects for Beyond-visual-line-of-sight urban air mobility services, flying UAVs over futuristic smart cities, are coming to reality (GSMA, 2019). Such a situation requires UAVs with a strong degree of automation in order to avoid or at least minimize possible accidents, depending on several well known flight control systems on board the aircraft. However, the increasing number of UAVs is being accompanied by the development of 5G-and-Beyond communications networks. Thus, it is expected that, in a short time, commercial UAVs might become some sort of mobile network client devices, like smartphones.

The communications network can be used to restrict UAV operations at specific areas. These restrictions could be related to safety (e.g., near an airport), security (near sensitive government installation), or privacy (flying over private property), in order to guarantee safe autonomous flight under local rules of aviation (GSMA, 2019).

In the futuristic configuration discussed, UAVs automatic control systems will then assume a distributed form, with part of the controllers on board the aircraft and part remote and integrated to the communications network, characterizing a feedback control system with delay and packet loss. These will operate by sending control command data and receiving sensor data by means of a communication system common to various clients in the same network, so the demand on such network may adversely affect its quality and consequently the stability of the control systems which depend on the network's performance.

The increase in the delay adversely interferes in the stability margins of the control-loop, which can lead to instability and the consequent accident of the UAV. For this reason it is fundamental the study of effective control techniques for delay compensation and capable of guaranteeing robust stability margins. Also, since it is considered as a network distributed control problem of an ever-increasing number of UAVs, the simplicity and reliability are of paramount importance, thus requiring the priority investigation of control techniques widely applied to industrial systems.

In this context we propose to investigate the application of a Smith predictor-based adaptive Proportional-Integral-Derivative (PID) control due to its solid acceptance as a trustworthy industrial technique. The Smith predictor can mitigate the network's latency effects and supply the feedback control-loop with estimated data whenever

sensor data packets get lost (Hotchi et al., 2020; Sarkar et al., 2020). The PID with Smith predictor topology is well understood within the process control industry and within the control theory literature, allowing both analytical and experimental assessment of the robustness margins (Franklin and Santos, 2020).

The approach to be covered in this paper is to assess a computationally inexpensive and robust control solution to attend a great number of UAV clients of a futuristic flight control network, serving as a low level guidance system, possibly to work along with machine decision systems on top of it. In this context, intelligent artificial systems would monitor the need to interfere in controlling UAVs but the feedback control of 3D (three dimensional) position and velocity of network-controlled UAVs would be conducted by the Smith predictor-based adaptive control system. In this sense, guidance, navigation and control systems (GNC) are distributed among the network and UAVs, and are required to adapt in real-time due to mobility, atmospheric disturbances and different vehicle's dynamics.

Adaptive control techniques have been vastly applied in industrial process control (Astrom and Wittenmark, 2008). The baseline for such systems is the least-squares parametric estimation in the recursive and non-recursive forms, in most cases. One particular similarity between networked UAV control and some industrial process control is the existence of time delays in the control-loop. Such a delay is associated to the time a control command takes to modify the process output and the time the sensor data takes to be fed back to the controller. In the UAV case the total delay might be further increased due to signal processing stages and network traffic.

In Fig. 1 we show a simplified diagram of a network-controlled quadrotor system. Observe the network environment, in the middle, between the quadrotor and a remote computer station. Such environment is a non-linear and time-varying dynamical system dependent on so many considerations that we must left aside in order to keep in the planned track of this work. The Quadrotor block is also an extremely complex dynamic system. Thus, to view such combined complex systems from the perspective of control system design, we assume the combination as depicted by the single Networked-Quadrotor Dynamics block, modeled as a multi-input multi-output (MIMO) process with a bounded maximum time delay.

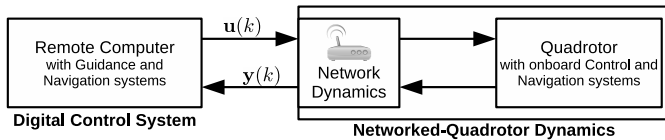


Figure 1. Block diagram of an autonomous networked-quadrotor control system.

Within the considered scenario we propose to contribute by presenting the following experiments:

- Assess a Smith predictor-based approach to deal with networked control of UAV under time delay and packet loss.

- Evaluate how the Smith predictor deals with stochastic disturbances affecting the UAV 3D position and velocity.
- Analyze how the proposed adaptive control approach adapts within the considered scenario and how it manages robustness assessment in real-time when the network's performance degrades.

Beyond this introductory part this paper is organized as follows: in Section 2 a Networked-Quadrotor MIMO process is described and the 3D position and velocity control problems are presented; in Section 3 the Smith predictor approach is discussed and followed by the digital self-tuning PID controller and its robustness assessment; in Section 4, simulations are assessed comparing the proposed control approach in face of conventional self-tuning PID; the adaptive control robustness is evaluated and confirmed under stochastic disturbances, increased network latency and packet loss; finishing with the Conclusions.

2. NETWORK-CONTROLLED UAV MODEL

Consider the non-singular, controllable and observable quadrotor's MIMO discrete-time stochastic system model

$$x(k) = Ax(k-1) + Bu(k-d) + \Gamma w(k-1), \quad (1)$$

$$y(k) = Cx(k) + v(k), \quad (2)$$

where $x(k) \in \mathbb{R}^n$ is the vector of n state variables, $u(k) \in \mathbb{R}^{n_u}$ is the vector of n_u inputs, $y(k) \in \mathbb{R}^{n_y}$ of n_y outputs, $w(k) \in \mathbb{R}^n$ and $v(k) \in \mathbb{R}^{n_y}$ are Gaussian disturbance vectors with respectively $\sigma_{w_1}^2, \dots, \sigma_{w_n}^2$ and $\sigma_{v_1}^2, \dots, \sigma_{v_{n_y}}^2$ variances. The $A \in \mathbb{R}^{n \times n}$, $B \in \mathbb{R}^{n \times n_u}$, $C \in \mathbb{R}^{n_y \times n}$, $\Gamma \in \mathbb{R}^{n \times n}$ are the matrices of the system and $d \geq 1$ is the discrete-time delay.

Equations (1) and (2) describe part of the simulation model of the UAV considered in this work. Its parameters are available in the work of Silveira et al. (2020) respective to the UAV's dynamics from the perspective of a remote control station as depicted in Fig. 1. The system's state vector is comprised of eight state variables,

$$x^T = [\phi \ \theta \ u_{vel} \ v_{vel} \ \psi \ r \ h \ w_{vel}], \quad (3)$$

designating, from left to right, the roll angle [rad], pitch angle [rad], vehicle's longitudinal velocity [m/s], lateral velocity [m/s], compass heading/yaw angle [rad], yaw rate [rad/s], altitude [m] and vertical velocity [m/s].

The time delay d in (1) is time-varying but assumed to be known and bounded. Also, control commands and sensor data have a probability P_{loss} of getting lost. In case of data sample loss, last data is repeated: $y(k) = y(k-1)$. The sampling time is fixed at 65 ms.

The UAV body-fixed orientation adopted is the $\bar{x}, \bar{y}, \bar{z}$ axes in the North-East-Down NED system, in which a right-handed rotation about the \bar{x} -axis gives positive roll; about the \bar{y} -axis gives positive pitch; about the \bar{z} -axis gives positive yaw (Stevens et al., 2016).

The input vector of the system in (1) is given by

$$u^T = [u_v \ u_u \ u_\psi \ u_w], \quad (4)$$

where all inputs are dimensionless and defined in the range of $[-1, 1]$. These inputs are respective to, from left to right: the lateral thrust, longitudinal thrust, yaw thrust and vertical thrust.

The MIMO networked-quadrotor control system considered encompasses six subsystems indexed by $i = 1, \dots, 6$. The first four are directly actuated by (4) and, in order, define the following control problems: 1. body-fixed lateral velocity ($y_1 = v_{vel}$) control, 2. body-fixed longitudinal velocity ($y_2 = u_{vel}$) control, 3. yaw angle ($y_3 = \psi$) control and 4. altitude ($y_4 = h$) control. The remainder two are cascade control problems, posed as outer loops dependent on the first two and defined as: 5. longitude position ($y_5 = p_{lon}$) control, 6. latitude position ($y_6 = p_{lat}$) control.

The design of all $i = 1, \dots, 6$ control systems are based on single-input, single-output, time-varying, estimated transfer function models, $G_i(k, z^{-1})$, of the form

$$A_i(k, z^{-1})Y_i(z^{-1}) = B_i(k, z^{-1})z^{-d}U_i(z^{-1}), \quad (5)$$

$$A_i(k, z^{-1}) = 1 + a_{i_1}(k)z^{-1} + \dots + a_{i_{n_a}}(k)z^{-n_a}, \quad (6)$$

$$B_i(k, z^{-1}) = b_{i_0}(k) + b_{i_1}(k)z^{-1} + \dots + b_{i_{n_b}}(k)z^{-n_b}, \quad (7)$$

where $Y_i(z^{-1})$ refers to the outputs and $U_i(z^{-1})$ to the inputs, both subjected to time-varying $A_i(k, z^{-1})$ and $B_i(k, z^{-1})$ polynomials defined in the backward shift operator domain, z^{-1} . The polynomials in (5) are estimated online and on demand by the respective $i = 1, \dots, 6$ adaptive controllers. Thus, (1) and (2) define the body-fixed simulation model and (5) the controller design model.

A navigation system model is required in order to allow the UAV position control with respect to an external fixed reference frame, i.e., the Earth. By integrating the velocities given in terms of the external fixed reference frame we can obtain the longitude and latitude position of the UAV. In Fig. 2 we present how the quadrotor's NED body-fixed velocities can be decomposed into an Earth-fixed Cartesian longitude and latitude coordinate system.

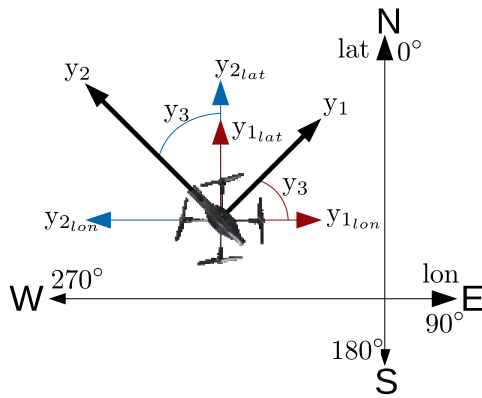


Figure 2. Quadrotor's North-East-Down body system velocities with respect to a Cartesian latitude and longitude coordinate system.

From the diagram in Fig. 2 a transformation matrix dependent on the compass heading angle $y_3 = \psi$ can be obtained:

$$M = \begin{bmatrix} \cos[y_3(k)] & \sin[y_3(k)] \\ -\sin[y_3(k)] & \cos[y_3(k)] \end{bmatrix}. \quad (8)$$

Then, body-fixed velocities can be converted into Earth's reference frame velocities, longitudinal (v_{lon}) and latitudinal (v_{lat}), given by:

$$\mathbf{v}_E(k) = \begin{bmatrix} v_{lon}(k) \\ v_{lat}(k) \end{bmatrix} = M \begin{bmatrix} y_1(k) \\ y_2(k) \end{bmatrix} \quad (9)$$

The inverse of the transformation matrix M ,

$$M^{-1} = \begin{bmatrix} \cos[y_3(k)] & -\sin[y_3(k)] \\ \sin[y_3(k)] & \cos[y_3(k)] \end{bmatrix}, \quad (10)$$

can be used to obtain the corresponding body system velocities from Earth's Cartesian coordinate system:

$$\begin{bmatrix} y_1(k) \\ y_2(k) \end{bmatrix} = M^{-1} \begin{bmatrix} v_{lon}(k) \\ v_{lat}(k) \end{bmatrix} \quad (11)$$

By applying the Backward difference approximation to the problem of integrating velocities in order to obtain the position, the UAV position given in Earth's reference system, \mathbf{p}_E , is incremented based on updated velocities:

$$\mathbf{p}_E(k) = \begin{bmatrix} p_{lon}(k) \\ p_{lat}(k) \end{bmatrix} = \mathbf{p}_E(k-1) + T_s \mathbf{v}_E(k), \quad (12)$$

where $y_5 = p_{lon}$, $y_6 = p_{lat}$ and T_s is the sampling time in use within the guidance and navigation systems.

Equations (8) to (12) can also be used to transform 3D position reference information from Earth's coordinate system to the body-fixed coordinate system and vice-versa in order to be used as reference signals for the guidance controllers.

3. SMITH PREDICTOR-BASED ADAPTIVE CONTROL

In the 1950s Otto J. M. Smith proposed a closed-loop predictor structure for open-loop-stable processes as depicted in Figure 3. The key element in Smith's structure was the simplicity in which a delay-free observer $\bar{G}_i(z^{-1})$ was used in order to produce a predicted output $\hat{y}_i(k+d)$. Then, ideally, the controller $C_i(z^{-1})$ would work d -steps ahead so to move $\hat{y}_i(k+d)$ towards the reference $r_i(k)$. And, if the main difference between the observer and the real process $G_i(z^{-1})$ is the time delay, then the prediction error $e_{p_i}(k) = y_i(k) - \hat{y}_i(k)$ would be null, leading to the compensation of the delay's effects on the closed-loop stability margins.

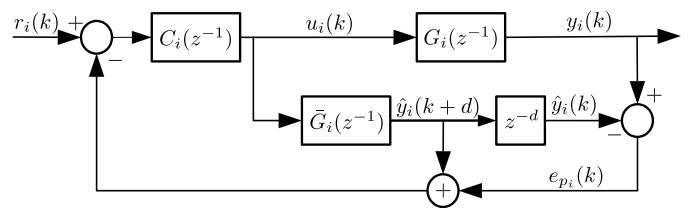


Figure 3. Block diagram of a PID control-loop with the Smith Predictor.

Assuming the parameters from (5) could be estimated online and that d is an accessible network parameter, then a delay-free observer can be adapted in real-time so to cope with Smith's strategy. The recursive least-squares estimator was selected for this task since its application is straightforward:

$$L_i(k) = \frac{P_i(k-1)\phi_i(k)}{1 + \phi_i^T(k)P_i(k-1)\phi_i(k)}, \quad (13)$$

$$\theta_i(k) = \theta_i(k-1) + L_i(k) [y_i(k) - \phi_i^T(k)\theta_i(k-1)], \quad (14)$$

$$P_i(k) = [I - L_i(k)\phi_i^T(k)] P_i(k-1). \quad (15)$$

These last three equations are respective to the estimator's gain, parameters vector and the estimation error covariance matrix. Present in all these equations is $\phi_i(k)$, known as the vector of output and input regressors. Smith's predicted output may also have its own $\hat{\phi}_i(k)$ adopting non-delayed input regressors and the most recent estimated parameters, such that

$$\hat{y}_i(k+d) = \hat{\phi}_i^T(k)\theta_i(k) \quad (16)$$

Thus, these results can be directly applied to the control strategy as it follows:

$$u_i(k) = C_i(k, z^{-1})e_i(k) \quad (17)$$

$$e_i(k) = r_i(k) - y_i(k) + \hat{y}_i(k) - \hat{y}_i(k+d) \quad (18)$$

Considering the PID control law in the continuous frequency domain and in its parallel form,

$$U_i(s) = \left(K_{i_P} + \frac{K_{i_I}}{s} + K_{i_D}s \right) E_i(s). \quad (19)$$

K_{i_P} , K_{i_I} , K_{i_D} , are, respectively, the proportional gain, the integral and derivative gains, used to tune the control-loop. By applying the Backward-difference approximation $s := (1 - z^{-1})/T_s$ to (19), the following digital PID is defined:

$$U_i(z^{-1}) = \frac{(s_{i_0} + s_{i_1}z^{-1} + s_{i_2}z^{-2})}{(1 - z^{-1})} E_i(z^{-1}) \quad (20)$$

$$\begin{aligned} s_{i_0} &= K_{i_P} + K_{i_I}T_s + \frac{K_{i_D}}{T_s} \\ s_{i_1} &= -K_{i_P} - 2\frac{K_{i_D}}{T_s} \\ s_{i_2} &= \frac{K_{i_D}}{T_s} \end{aligned} \quad (21)$$

In order to adapt $C_i(k, z^{-1})$, a model-based tuning presented by Castro et al. (2019) is considered. The method applies only for open-loop stable systems and consists in adapting the controller so to guarantee the following closed-loop reference model dynamics:

$$\frac{Y_i(z^{-1})}{R_i(z^{-1})} = \frac{(1 - e^{-\frac{T_s}{\tau_i}})z^{-1}}{1 - e^{-\frac{T_s}{\tau_i}}z^{-1}}. \quad (22)$$

The free parameter is τ_i , that corresponds to the time constant or the cut-off frequency $\omega_i = 1/\tau_i$ of the system in (22). This tuning technique is based on a second-order discrete-time system model and it is self-tuned after $\theta_i(k) = [a_{i_1}(k) \ a_{i_2}(k) \ b_{i_0}(k) \ b_{i_1}(k)]^T$ innovations:

$$\begin{aligned} s_{i_0}(k) &= \frac{1 - e^{-\frac{T_s}{\tau_i}}}{b_{i_0}(k) + b_{i_1}(k)} \\ s_{i_1}(k) &= s_{i_0}(k)a_{i_1}(k) \\ s_{i_2}(k) &= s_{i_0}(k)a_{i_2}(k) \end{aligned} \quad (23)$$

Alternatively, the adaptive PID gains are as follows:

$$\begin{aligned} K_{i_P}(k) &= -s_{i_1}(k) - 2s_{i_2}(k) \\ K_{i_I}(k) &= \frac{s_{i_0}(k) + s_{i_1}(k) + s_{i_2}(k)}{T_s} \\ K_{i_D}(k) &= s_{i_2}(k)T_s \end{aligned} \quad (24)$$

Among the six $i = 1, \dots, 6$ control systems, the last two were linked in a cascaded manner as outer loops around

the first two. In this sense, the outputs of (12) are fed back to the following guidance proportional controller:

$$\begin{bmatrix} u_5(k) \\ u_6(k) \end{bmatrix} = \begin{bmatrix} K_{5_P} \\ K_{6_P} \end{bmatrix} M^{-1} \begin{bmatrix} r_5(k) - y_5(k) \\ r_6(k) - y_6(k) \end{bmatrix}. \quad (25)$$

Their control signals serve, in fact, as reference signals to the body-fixed lateral and longitudinal controllers: $[r_1(k) \ r_2(k)]^T = [u_5(k) \ u_6(k)]^T$.

Since self-tuning controllers adapt in real-time, then stability and robustness analyses must accompany and adapt as well. However, frequency domain analysis towards asymptotic stability verification or gain and phase margins calculations in real-time may require specialized software development libraries and more computer processing power and memory. Thus, a time-based robustness index for self-tuning control is considered (Silveira et al., 2012):

$$R_{I_i}(k) = \frac{\left| \frac{\sum_{j=0}^k \hat{y}_i(j) - \sum_{j=0}^k y_i(j)}{\sum_{j=0}^k \hat{y}_i(j) \sum_{j=0}^k S_i(k, z^{-1})r_i(j)} \right|}{\left| \frac{\sum_{j=0}^k S_i(k, z^{-1})y_i(j)}{\sum_{j=0}^k S_i(k, z^{-1})r_i(j)} \right|}, \quad (26)$$

where $S_i(k, z^{-1})$ is a time varying polynomial comprised of the elements shown in (23). If $R_{I_i}(k) < 1$, then the adaptive control-loop is said to be robust at time k .

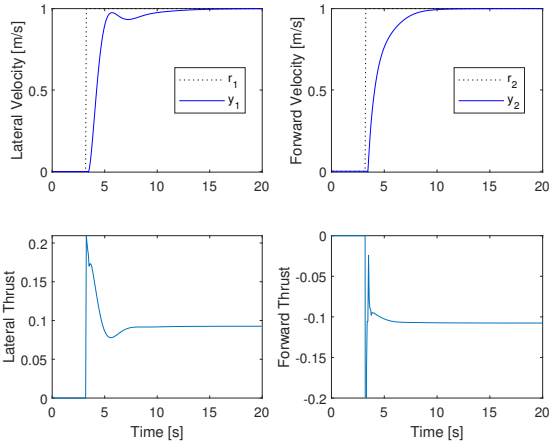
4. SIMULATIONS RESULTS

To refer to the Smith predictor-based adaptive controller, the acronym SPAC will be used henceforth.

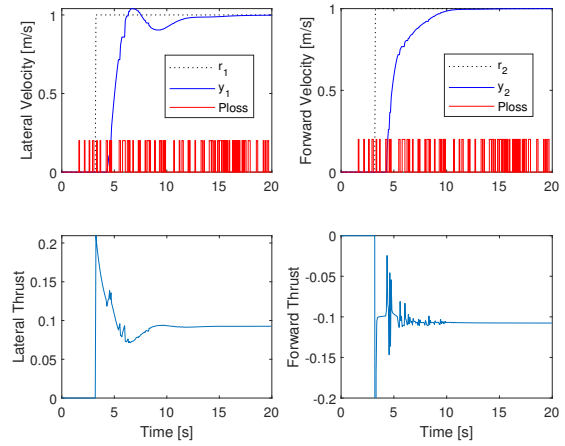
The first four controllers were tuned using $[\tau_1 \ \tau_2 \ \tau_3 \ \tau_4] = [1 \ 1 \ 3.6 \ 1.3]$. Initial covariance matrices P_i and parameters θ_i were estimated and used to initialize the SPAC and then its PID gains were adapted in real-time so to force the closed-loop system to behave as in (22), while the other two guidance systems were set with $[K_{5_P} \ K_{6_P}] = [1 \ 1]$. The nominal time delay of the UAV was 195 ms ($d = 3$) when the network performance was also nominal. In a worst case scenario it was assumed a maximum time delay of 975 ms ($d = 15$) and a packet dropout probability of 30% along with atmospheric disturbances and sensor noise, as modeled in Silveira et al. (2020).

SPAC τ_i 's were tuned after evaluations of the step responses in the nominal scenario. In Fig. 4 it is shown the step responses and the control signals for the $i = 1, 2, 3, 4$ systems. The selected τ_i 's guarantee that all control signals respect the saturation limits of $[-1, 1]$ when an abrupt step-like reference is required. However, it is important to highlight that the guidance system controls the UAV from a departure waypoint to the next along a predefined trajectory, like an airway, so the step-like references may be abrupt but of small values, since the planned path is supposedly to be continuous between waypoints.

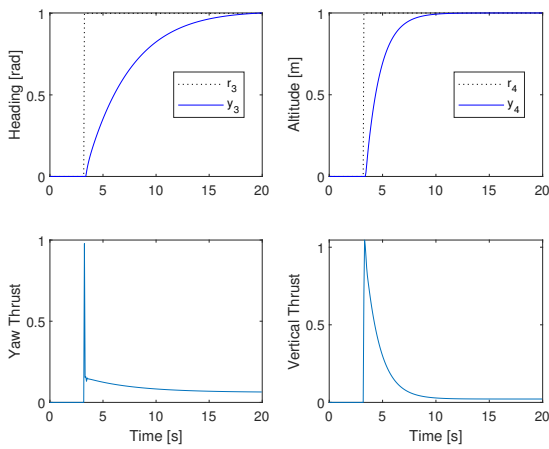
The SPAC closed-loop behavior was also assessed in a more complex scenario of 975 ms delay ($d = 15$) and with a packet dropout probability of 30%. The results are shown in Fig. 5, where it is possible to observe that, despite the adverse scenario, the controller handled its task robustly, as confirmed in Fig. 6 where all R_{I_i} , $i = 1, 2, 3, 4$, were kept



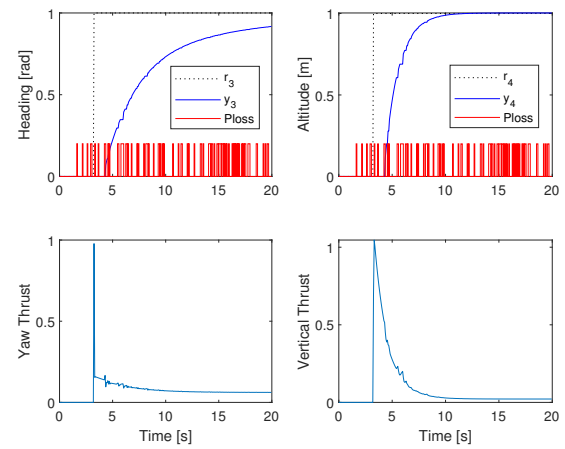
(a) UAV velocities control.



(a) UAV velocities control.



(b) UAV heading and altitude control.



(b) UAV heading and altitude control.

Figure 4. SPAC assessed in the nominal scenario.

below the unity threshold. On the other hand, in Fig. 7, a similar adaptive PID, but without SPAC, exhibited stability degradation with highly oscillatory lateral and longitudinal velocities.

The SPAC was also assessed in a 3D trajectory tracking essay under the worst case scenario, which incorporates atmospheric disturbances and sensor noise, along with the previous evaluated case of 975 ms delay and packet dropout probability of 30%. The planned reference trajectory was an ascending spiral since it poses some additional difficulties than tracking straight lines. The results are shown in Fig. 8, where in (a) the 3D trajectory tracking is nominal and (b) it is in worst case scenario. In this last case, during the initial phase of the mission, the UAV trajectory dispersion was large since SPAC was still adapting. However, in the long run, SPAC proved to be stable and robust. The result without SPAC is not shown due to space limitations, but the UAV became unstable under simulated atmospheric disturbances along with the 975 ms time delay and 30% packet loss probability.

CONCLUSIONS

In this work, a Smith predictor-based adaptive GNC system was investigated with focus on network-controlled

Figure 5. SPAC under 975 ms time delay and 30% packet loss probability (red spikes denote packet drops).

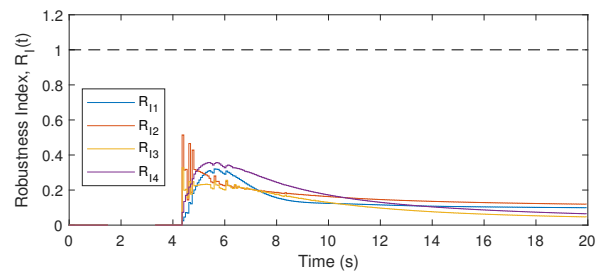
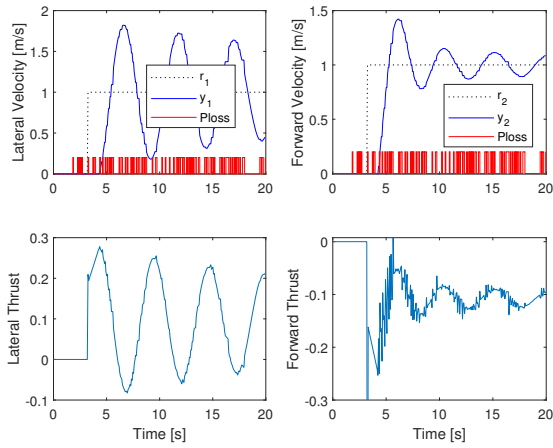
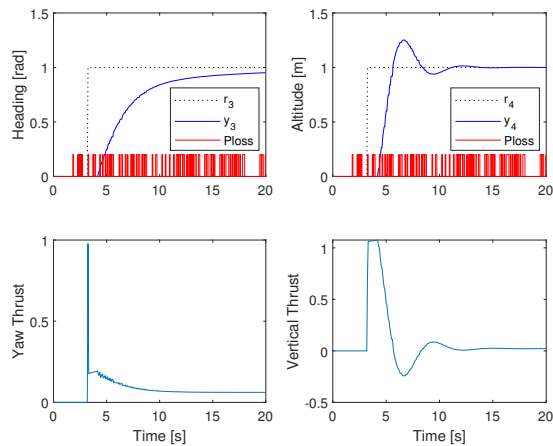


Figure 6. SPACs robustness indices (975 ms time delay and 30% packet loss probability).

UAVs. It was assumed a futuristic scenario of an ever increasing number of aerial vehicles in populated zones, all within a supervised flight control network dependent on the communications network performance. The proposed control approach was based on reliable industrial techniques, such as the Smith predictor and self-tuning PID control, so to cope with a trustworthy and computationally inexpensive approach. The average loop-time of the complete GNC for a single UAV was 0.23 ms. The algorithm was tested with MATLAB R2018a in Ubuntu 18.04.5 LTS on an Intel i5-4200U CPU 1.60GHz and 4GB RAM. The



(a) UAV velocities control without SPAC.



(b) UAV heading and altitude control without SPAC.

Figure 7. Without SPAC, 975 ms time delay and 30% packet loss probability (red spikes denote packet drops).

simulated results confirmed the proposed GNC system to be robust under the complex scenario of increased time delay, packet dropout probability of 30% and robust to atmospheric and sensor noise disturbances.

REFERENCES

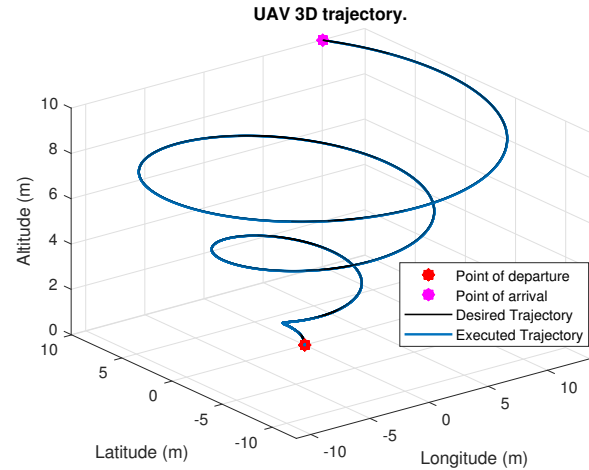
Astrom, K.J. and Wittenmark, B. (2008). *Adaptive Control*. Dover Pub., Mineola, NY, USA, 2nd edition.

Castro, L., Filho, H., Amorim, G., and Silveira, A. (2019). Design of pid type local controller network with fuzzy supervision. *IEEE Latin America Transactions*, 17(05), 759–765.

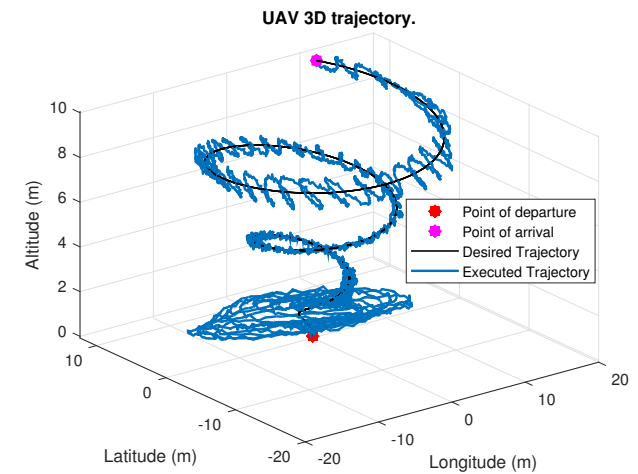
Franklin, T.S. and Santos, T.L. (2020). Robust filtered smith predictor for processes with time-varying delay: A simplified stability approach. *European Journal of Control*, 56, 38–50.

GSMA (2019). *Mobile-Enabled Unmanned Aircraft*. <http://www.gsma.com/iot/wp-content/uploads/2018/02/Mobile-Enabled-Unmanned-Aircraft-web.pdf>. Accessed on June 7, 2021.

Hotchi, R., Chibana, H., Iwai, T., and Kubo, R. (2020). Active queue management supporting tcp flows using



(a) SPAC of UAV 3D trajectory: nominal scenario.



(b) SPAC of UAV 3D trajectory: worst scenario.

Figure 8. SPAC of UAV 3D trajectory in (a) nominal and (b) in adverse worst scenario with atmospheric disturbances, sensor noise, 975 ms delay and 30% of packet dropout probability.

disturbance observer and smith predictor. *IEEE Access*, 8, 173401–173413.

Sarkar, M., Subudhi, B., and Ghosh, S. (2020). Unified smith predictor based h_∞ wide-area damping controller to improve the control resiliency to communication failure. *IEEE/CAA Journal of Automatica Sinica*, 7(2), 584–596.

Silveira, A., Silva, A., Coelho, A., Real, J., and Silva, O. (2020). Design and real-time implementation of a wireless autopilot using multivariable predictive generalized minimum variance control in the state-space. *Aerospace Science and Technology*, 105, 106053.

Silveira, A.S., Rodríguez, J.E., and Coelho, A.A. (2012). Robust design of a 2-dof gmvc controller: A direct self-tuning and fuzzy scheduling approach. *ISA Transactions*, 51(1), 13–21.

Stevens, B.L., Lewis, F.L., and Johnson, E.N. (2016). *Aircraft Control and Simulation: dynamics, controls design, and autonomous systems*. John Wiley & Sons, Inc., 3rd edition.